Mesoporous Materials as Templates for Semiconductor Nanowire Assembly

Justin D. Holmes*, Michael A. Morris and Kevin M. Ryan

[1]*Department of Chemistry, Materials Section and Supercritical Fluid Centre, University College Cork, Cork, Ireland.*

**To whom correspondence should be addressed: Telephone: +353 (0)21 4903608; Fax : +353 (0)21 4274097, E-mail: j.holmes@ucc.ie*

Abstract

In this chapter is described a novel approach for synthesizing mesoporous silicas with tunable pore diameters, wall thickness and pore spacings that can be used as templates for the assembly of semiconductor nanowire arrays. Silicon and germanium nanowires, with size monodisperse diameters, can readily be formed within the mesoporous silica matrix using a supercritical fluid inclusion technique. These nano-composite materials display unique optical properties such as intense room temperature ultraviolet and visible photoluminescence. The implication of these mesoporous nanowire materials for future electronic and opto-electronic devices is discussed.

Keywords: Nanowires, Mesoporous Silica, Supercritical Fluid.

Introduction

Many technologies, including electronics, separation science and coatings will be enhanced by the ability to control the structure of materials on a nanometer-length scale. The ability to pack high densities of memory storage and processing circuitry into specific nanoscale arrays, and utilise the unique transport properties associated with these architectures, is expected to lead to future generations of (nano)-computer processors with device sizes many times smaller and faster than current silicon based processors[1]. However, both physical constraints and economics are expected to limit continued miniaturization of electronic and optical devices using current 'top-down' lithography based methods[2]. Consequently, alternative non-lithographic methodologies for constructing the smallest mesoscopic features of an integrated circuit will soon be needed. One promising non-lithographic strategy for creating mesoscopic architectures is the use of solution phase chemistry to assemble materials from precursor 'building block' into structurally complex mesoscopic architectures[3].

One dimensional (1D) structures, or nanowires, have great potential as building-blocks for the 'bottom-up' assembly of nanoscale structures as they can function as both devices and as the conducting wires that access them. Several groups have demonstrated that carrier type (electrons, n-type; holes, p-type) and carrier concentrations in single crystal silicon nanowires can be controlled during growth using phosphorous and boron dopants[4,5]. Additionally for low-dimensional semiconductors, quantum effects due to spatial confinement may give rise to novel and unusual properties such as tunable photoluminescence (PL). In particular, the discovery of visible luminescence from nanocrystalline silicon has led to an explosion of interest in this material for potential opto-electronic applications[6]. A number of techniques for preparing pseudo- 1D wires have been reported including laser ablation of silicon and germanium targets[7], liquid crystal templating methods and vapour-liquid-solid growth mechanisms[8]. We have been instrumental in developing a novel supercritical fluid (SCF) solution–phase technique for producing silicon nanowires with tunable crystal orientation and hence controllable optical properties[9].

Even though the preparation of semiconductor nanowires in bulk quantities is now possible, unanswered questions relating to their processibility remain. Nearly all of the routes for synthesizing nanowires described above typically yield disordered entanglements of nanowires which have limited usefulness. Encapsulation of nanowires within an ordered template offers the possibility of manipulating nanowires into useful configurations and allows their aspect ratios, and hence their physical properties, to be tailored. Nanometre-wide channels of anodic aluminium oxide films[10,11], polycarbonate track etched membranes[12] and nanochannel array glasses[13] have previously been used as templates for nanowires of conductive polymers[14], metals[15], and semiconductors[16]. Whilst these templating methods are useful, forming an ordered array of nanoscale channels within these templates is difficult and the channel dimensions are usually too large to engineer nanowires that exhibit useful quantum confinement effects.

Significantly, mesoporous solids[17] that contain uni-directional arrays of pores, typically 2-15 nm in diameter, running throughout the material have been successfully exploited as templates for semiconductor nanoclusters formed from the gas-phase. In particular, Leon *et. al.* [18] reported the partial filling of MCM-41 mesoporous silica with germanium wires using vapor-phase epitaxy. In a similar approach Dag *et. al.* [19] employed chemical vapor deposition (CVD) to deposit silicon nanocrystals within the pores of hexagonal mesoporous films. Certainly, these gas-phase methods have yielded high quality semiconductor nanomaterials but the high temperatures, *ca.* 800 °C, or extensive reaction times, *ca.* 48 hours, often required for successful nucleation and growth of the materials within the mesopores makes these techniques both costly and time-consuming. Recently we have reported the use of a novel supercritical fluid (SCF) inclusion technique to produce silicon and germanium nanowires within the pores of mesoporous silica 'powders' to form semiconductor nanowire arrays[20-22]. The high-diffusivity of the SCF[23] and the very high gas pressures which overcome surface tension at the pore openings enables the rapid transport of the semiconductor precursor into the mesopores of the silica thereby allowing swift nucleation and growth and reducing the reaction time for pore filling by at least an order of magnitude compared to chemical vapour deposition (CVD).

In this paper we describe in detail the use of non-ionic triblock copolymer surfactants to template the formation of ordered hexagonal mesoporous silica materials and the use of SCF methods to reproducibly form a range of tailor-made high quality silica-nanowire composites with unique optical properties.

Mesoporous Silica Preparation

The use of triblock copolymer surfactants has been widely adopted in the synthesis of stable mesoporous silicas[24]. The mesoporous silica samples synthesized in our experiments were prepared using a novel preparation in which a surfactant concentration, 50 wt%, was used as a hexagonal template. This preparation is similar to the liquid crystal templating method used by Attard et al**.** [25] to prepare mesoporous silicas from short chain polyethylene oxide based surfactants.

Hexagonal mesoporous silicas were prepared by the acid hydrolysis of tetramethoxysilane (TMOS) in the presence of poly(ethylene oxide) (PEO) – poly(propylene oxide) (PPO) triblock copolymer surfactants, *e.g.* P85 ($PEO_{26}PPO_{39}PEO_{26}$), P123 ($PEO_{20}PPO_{69}PEO_{20}$), P65 ($PEO_{20}PPO_{30}PEO_{20}$) or mixtures of these surfactants. The surfactants used were supplied by Uniquema, Belgium. In a typical synthesis a mixture of P85 (0.5 g) was dissolved in TMOS (1.8 g, 0.0118 mol) and added to an aqueous solution of HCl (1 g, 0.5 M) to give a surfactant concentration of 50 wt%. Methanol generated during the reaction was removed on a rotary film evaporator at 40°C. The resulting viscous gel was left to condense at 40°C for one week in a sealed flask. Calcination of the condensed gel was carried out in air for 24 hr at 450°C. Any residual surfactant was removed by flowing a 5 % ozone stream (Yanco Ozone Generator GE60/MF 5000) over the silica for 30 minutes. Powder X-ray diffraction (PXRD), transmission electron microscopy (TEM) and nitrogen adsorption techniques were used to establish pore diameters, silica wall widths and the hexagonal packing of the pores within the calcined silicas.

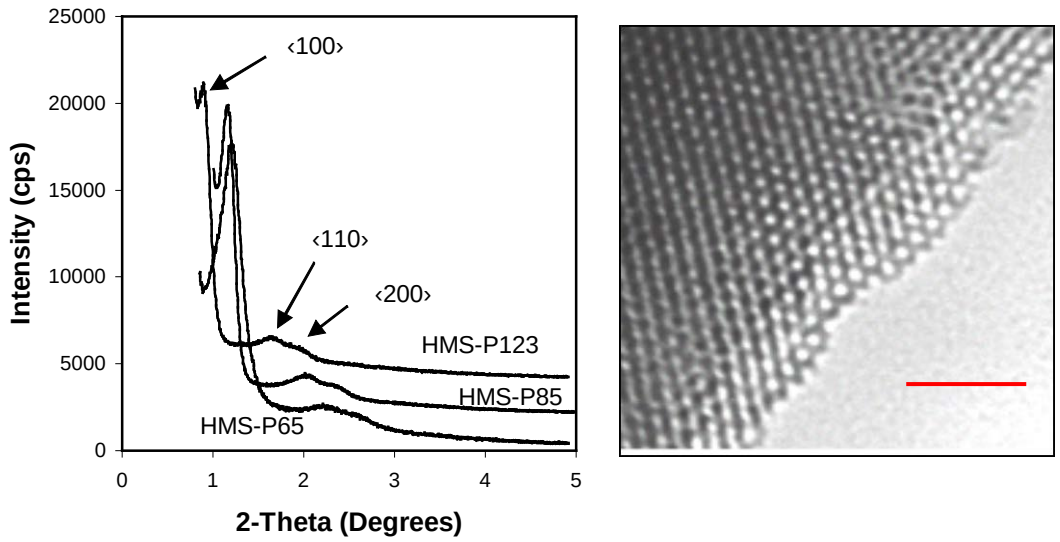

Figure 1. (a) Low angle PXRD data collected for a series of hexagonal mesoporous silicas prepared using P65, P85 and P123 triblock copolymer surfactants. (b) Transmission electron micrograph of P85. (Scale bar represents 50 nm).

Low angle powder X-ray diffraction (PXRD) data for calcined hexagonal mesoporous silica materials synthesised from P65, P85 and P123 triblock copolymer surfactants are shown in figure 1a. For all of the mesoporous silica templates synthesised, intense features were observed, and are indexed in the figure as the <100>, <110> and

<200> reflections. These features are consistent with highly ordered long-range mesoporous arrays with a repeat distance of 72 Å, 76 Å and 98 Å for P65, P85 and P123 respectively based on the position of the <100> reflection, and corresponding to pore center-to-pore center distances of 83 Å, 88 Å and 113 Å[26]. Transmission electron micrographs allow direct observation of high quality mesoporous materials for all samples prior to embedding nanowires, as shown in figure 1b.

Recently we have developed a novel approach for synthesizing calcined mesoporous silicas with tunable pore sizes, wall thickness and pore spacings using mixtures of triblock co-polymer surfactants as hexagonal templating agents[27]. Table 1 below displays how, by changing the relative concentrations of binary mixtures (namely P123:P85, P123:P65 and P85:P65) of the surfactant molecular templates the diameters of the mesopores and the spacing between the pores can be tuned with Ångström-level precision between the size range of 45-70 Å and 75-100 Å respectively. In particular, increasing the proportion of P123 in the surfactant template, relative to P85 or P65, leads to an increased pore diameter. Thus the diameter of the mesopores appears to depend on the size of the PPO core with the PEO tails being encapsulated in the silica matrix. Table 1 also reveals how the widths of the silica walls remain relatively constant for the P123:P85 templated range of silicas. A trend towards smaller wall thickness was observed upon incorporation of increasing concentrations of the P65 co-polymer into the P85:P65 or P123:P65 blends.

Table 1 Pore size, wall thickness and pore centre-to-centre distances for calcined mesoporous silicas synthesized using the direct templating method determined by PXRD.

	P123:P85			P85:P65			P123:P65		
Ratio (%)	Center (Å)	Pore (Å)	Wall (Å)	Center (Å)	Pore (Å)	Wall (Å)	Center (Å)	Pore (Å)	Wall (Å)
100:0	100	70	30	85	50	35	100	70	30
80:20	97	61	36	83	47	36	95	68	27
60:40	94	58	36	81	48	33	89	65	25
40:60	91	58	33	79	47	32	84	63	21
20:80	89	54	35	77	47	30	79	61	18
0:100	85	50	35	75	46	30	74	46	30

Center = mean center-to-center hexagonal pore spacing (± 1 Å); Pore = mean pore diameter (± 1 Å); Wall = mean wall thickness (± 1 Å). Values based on measurements from three sample batches.

In effect, our method allows mesopore engineering without the need for the ad-hoc addition of swelling agents and co-surfactants. Using commercially available bulk triblock co-polymer surfactants ensures that our method of pore engineering is commercially viable for many industrial applications. The tailored silicas produced have strong pore walls, typical of triblock templated mesoporous solids, along with enhanced thermal and hydrothermal stability as previously reported[21]. While other methods report loss of long-range pore order after calcination, the degree of ordering in the mesoporous silicas reported in the present work is maintained over micrometre length scales.

Semiconductor Nanowire Formation

Semiconductor (Si and Ge) nanowires can readily be grown within the silica mesopores using a SCF inclusion technique. This technique involves the degradation of the nanowire precursor, *i.e.* diphenylsilane or diphenylgermane for Si or Ge nanowires respectively, at elevated temperatures and pressures[20-22]. In a typical preparation 0.5 g P85 is degassed at 200°C in nitrogen for 6 hours and then placed in a high-pressure titanium reaction cell under an oxygen-free nitrogen atmosphere. For silicon nanowire preparation diphenylsilane (0.022 mol, 4.05 ml) was placed in the reaction vessel. The high-pressure cell was attached, via a three-way valve, to a stainless steel high-pressure tube (~21 ml) equipped with a stainless steel piston. An Isco high-pressure pump (Isco Instruments, PA) was used to pump carbon dioxide into the back of the piston and displace oxygen-free anhydrous hexane into the reaction cell to the desired pressure (375 bar). The cell was placed in a tube furnace and heated to 500°C (± 1°C) using a platinum resistance thermometer and temperature controller. The reaction proceeded at these conditions for between 15 to 30 minutes. A schematic diagram of the apparatus is shown in figure 2 below.

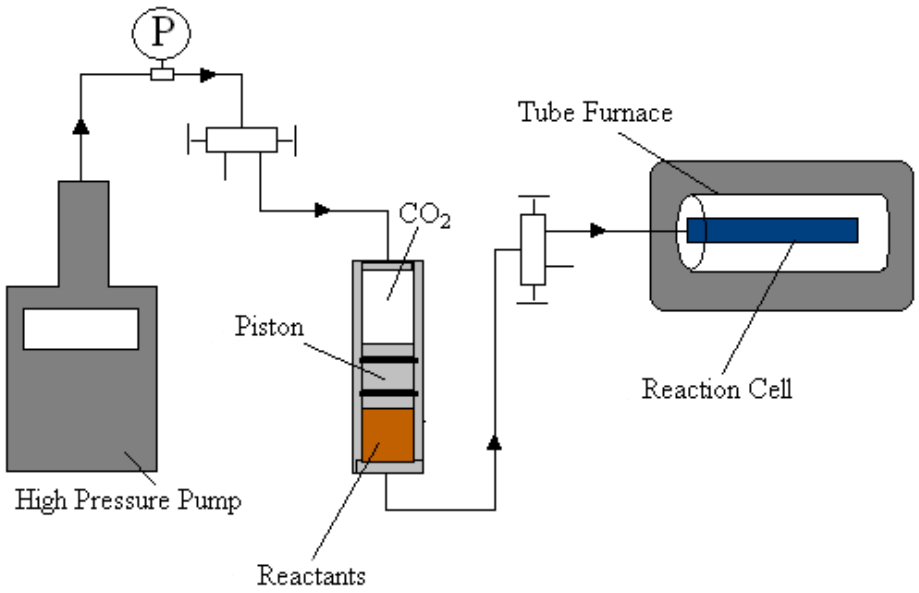

Figure 2 High-Pressure Apparatus schematic

The mesoporous silica changed color from white to dark orange/red for silicon and black for germanium during the course of the reaction. The end product was homogenous in appearance. No color change was observed in the absence of diphenylsilane (or diphenylgermane for Ge nanowire formation). After the reaction had finished the contents of the cell were washed out with hexane. The relatively large (~ 1 mm dimensions) particles of mesoporous silica incorporating silicon or germanium were collected from the reaction cell and washed in copious amounts of anhydrous hexane and ethanol prior to analysis.

Effectively, the silica mesopores act as templates for forming ordered arrays of nanowires, where the pore size of the silica dictates the diameter of the nanowires produced. ^{29}Si-MAS-NMR provides evidence for filling of the pores and binding of the

semiconductor nanowires to the pore walls of the silica. The ^{29}Si-MAS-NMR of mesoporous silica prior to nanowire inclusion shows two principle chemical shifts of –103.4 and –111.4 ppm, respectively assigned to species Q_3 ($Si(OSi)_3(OH)$) and Q_4 ($Si(OSi)_4$[19,28]. A smaller feature apparent at –92.4 ppm can be assigned to $Q_2(SiO_2(OH)_2)$ [19,28]. The Q_3 and Q_2 peaks result predominantly from species at the surface of the silica walls of each pore whereas Q_4 species are within the bulk silica walls. Upon silicon nanowire inclusion the loss of surface Si-OH site resonances and the formation of a Si_3(wall)-O-Si(wire) peak (-88.0 ppm) and a peak reminiscent of elemental silicon (Si_4Si) at -80.8 ppm infers that the nanowires are anchored to the surface of the mesoporous walls and pore-filling has been achieved. ^{29}Si MAS-NMR also revealed that the volume ratio of silicon and germanium to silica correlates to ~ 85-95 % of the mesopores being filled with silicon. Surface analyses by nitrogen sorption measurements was carried out on all the mesoporous silica and mesoporous silica-silicon/germanium nanowire composites synthesised. Prior to nanowire inclusion, the hexagonal mesoporous silicas displayed Type IV adsorption and desorption isotherms characteristic of mesoporous materials and had surface areas of 700-1000 m^2 g^{-1} calculated by the BET method. After nanowire inclusion in the pores, the surface area of all samples decreased by between 92 – 98 % of the original and the pore volume decreased by 96-99 % indicated that the mesopores are completely filled.

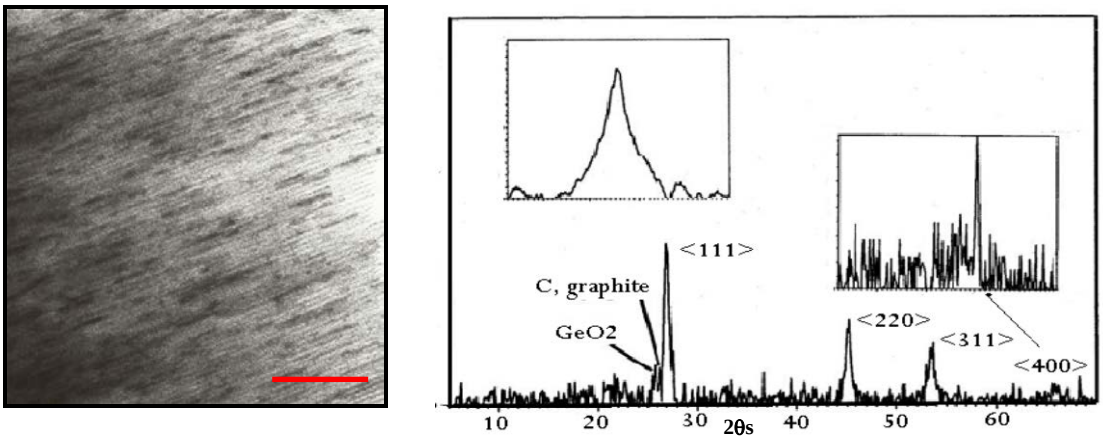

Figure 3 (a) TEM data showing germanium nanowires/nanorods incorporated inside the pores of a mesoporous silica sample (scale bar = 50 nm). (b) PXRD profile from germanium wires within mesoporous silica. Main reflections are indicated. The insert is the expansion of the <220> peak that shows a sharp feature (from planes perpendicular to the wire direction) superimposed on a broader peak (from planes parallel to the wire direction). The very sharp <400> feature suggests that the wires are aligned in the <100> direction.

It should be noted that there is no degradation of the mesoporous arrangement after nanowire inclusion as confirmed by PXRD and TEM which shows the mesoporous structure remains intact[21]. The nanowires formed are highly crystalline in nature. Data is shown in figure for germanium wires grown in identical conditions as silicon wires except using diphenylgermane as the precursor. The TEM data reveals the presence of features associated with crystalline germanium and detailed analysis of the features shows that the wires are orientated in the <100> direction within the silica pore system.

Unusual Optical Properties of Encased Silicon Nanowires

The origin of the PL in silicon nanowires is highly controversial. Many researchers argue that surface states[29] may be responsible for the visible light emission although the suggestion of other authors that the PL is an intrinsic property of silicon due to quantum confinement effects may be equally valid[30]. Others have argued that quantum confinement effects do not cause any PL in these systems[31]. Previous studies of silicon nanowires and nanoparticles[32] have attempted to probe the relationship between nanocrystal size and luminescence. We have reported on the PL emission properties of densely packed arrays of diametrically monodisperse cylindrical silicon nanowires confined within the pores of mesoporous silica. By nano-engineering of mesopore dimensions we successfully prepared silicon nanowires with diameters of 45 Å, 50 Å and 73 Å (± 10 %), and with lengths of > 1 μm[27]. The embedded nanowires displayed high monodispersivity, with narrow diameter distributions, allowing PL as a function of controlled crystallite diameter to be investigated.

Each silica-silicon nanowire composite prepared showed PL at wavelengths in both the visible-red and ultraviolet regions of the electromagnetic spectrum[33]. In our studies each nanowire-silica composite was interrogated at an excitation energy of 4.92 eV. Figure 4a shows that visible PL was observed for all of the nanowire samples at energies between 1.5-2.1 eV. PL emission maxima were observed at 1.79 eV and 2.01 eV for nanowires with 50 Å diameters (Si50) and emission at 1.98 eV and 2.05 eV for 45 Å diameter (Si45) nanowires.

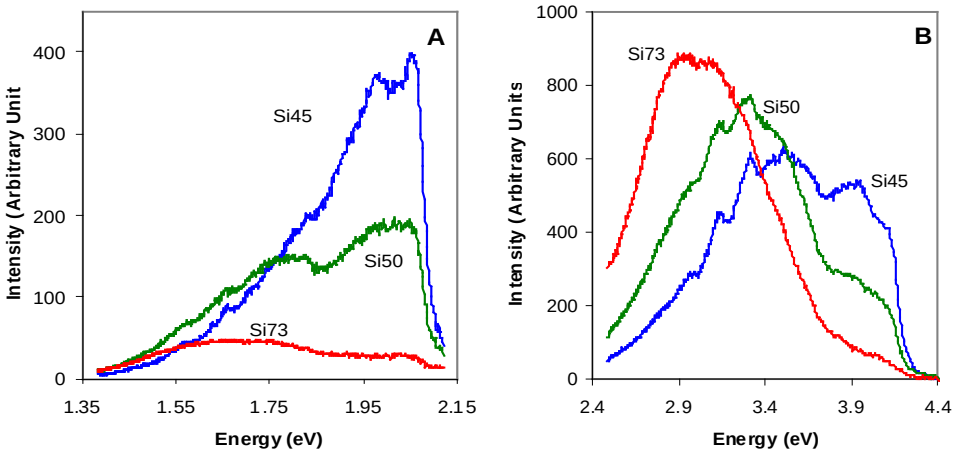

Figure 4 (a) Visible PL emission spectra for silicon nanowires embedded in a mesoporous silica matrix and dispersed in anhydrous hexane. (b) Ultraviolet PL emission spectra (excitation energy of 4.92 eV) collected for the same materials.

These two emission peaks are intrinsic to indirect-gap nanowires and are the slow band-edge emission band and the higher energy fast emission band respectively[34]. Figure 4b reveals the unusual high-energy PL emission peaks observed for the encapsulated silicon nanowire samples. Intense PL in the ultraviolet region of the electromagnetic spectrum was observed for all materials with a blue shift in the wavelength of the peaks as a function of decreasing nanowire diameter. Luminescence emission maxima were observed at 2.93 eV, 3.3 eV and 3.49 eV for Si73, Si50 and Si45 respectively. Hence, a linear decrease in emission wavelength with decreasing nanowire diameter was found. Smaller PL emissions

were observed at higher and lower energies than the PL emission peak maxima and mirrors discrete features that appear in the absorbance spectra.

PL in the ultraviolet region of the electromagnetic spectrum has been previously reported for both oxidised silicon nanowires[35] and completely amorphous silica nanowires[36]**.** The photo-physics properties of these systems have been ascribed to an electron-hole recombination model, where radiative recombination occurs at bulk silica defect centers arising from oxygen deficient sites such as two-fold co-ordinated silicon lone pair centers and neutral oxygen vacancies. However, for the silica-silicon nanowire composites prepared in our laboratories simply electron-hole recombination model does not explain the blue shift in the UV PL emission energy as the nanowire diameter decreases. Further it is difficult to rationalize the dramatic increases in PL yield that occur with relatively small decreases in wire diameter with a model based on the presence of surface defects. We have argued that this tunable UV PL arises from intrinsic 'strain effects' in quantum-sized nanocrystalline silicon[33]. Hence, as the nanowire diameter decreases, the strain induced in the backbonds from surface to internal silicon atoms also increases. These variations in surface state-derived band gap energies subsequently result in higher energy electronic transitions in strained nanocrystals than for bulk silicon[37]. Other authors such as Liu et al. [38] have reported stresses introduced to nanocrystalline silicon cores due to oxide shell growth may also alter the band structure, and hence the electronic properties, of nanocrystalline silicon.

This PL work demonstrates the ability to manipulate quantum confinement properties in 1-D semiconductor nanowires through strain induced surface states and offers experimental insight into a mechanism of light emission from nanocrystalline silicon that has not been widely investigated to date. The fabrication of such nano-scale composites offers new and exciting possibilities for a range of future opto-electronic applications and emerging technologies, from light emitting diodes to full colour intelligent image displays.

The Future of Templated Nanowire Assemblies

In summary, we have developed a unique SCF inclusion technique to fill the pores of a series of tailored hexagonal mesoporous silica, prepared using a contemporary surfactant templating method, with quantum confined semiconductor nanowires. Although not reported here, we have extended this method to form metal *e.g.* Co, Cu and metal oxide *e.g.* Fe_3O_4 nanowires within mesoporous silca matrices[39,40]. Unlike chemical vapour deposition techniques where the deposited material extends in almost all directions, promoting the growth of solid material across the tops of the pores and subsequent blocking of the pores, with our SCF method this is not observed. Furthermore the results presented in this chapter demonstrates the ability to manipulate quantum confinement properties in 1-D semiconductor nanowires offering experimental insight into a mechanism of light emission from nanocrystalline silicon that has not been widely investigated to date.

However, even though the mesoporous silica *powders* reported here have acted as ideal templates for growing quantum sized nanowires and have allowed us to probe their unique and unusual properties, for device application these mesoporous solids need to be cast as *films*. To date the formation of the nanowires within mesoporous films has not been reported, even though filling of the pores is an energetically favourable process and will likely result in uni-directional nanowire growth. Currently, we are attempting to synthesise two and three dimensional arrays of semiconductor, metal and metal oxide nanowires within mesoporous thin films that run both parallel or perpendicular to a substrate surface.

Additionally, while electronic functionality has been demonstrated in free-standing semiconductor nanowires[4], no comprehensive structural and electronic characterisation of our nanowire arrays has been undertaken to date. For example, transport mechanisms in semiconductor nanowires have not been investigated, *e.g.*, influence of wire structure and morphology (diameter, crystallinity, dopant and defect densities, interfacial properties, surface states, *etc*.) on measured nanowire device electrical parameters. Furthermore, no electrical contacting strategies have to date been employed to make connection to nanowires within mesopores. In terms of the development of opto-electronic devices Ng *et al*[41] have demonstrated that a silicon based LED can be fabricated. These mesoporous semiconductor nanowires could possibly be used to create arrays of point LEDs which have the capability of forming very high resolution screen displays a key component in the expansion of the information based technologies.

In conclusion, there is a lot of work required before mesoporous nanowires can be implemented in devices. However, the assembly of such nano-scale composites offers new and exciting possibilities for a range of future opto-electronic applications and emerging technologies, from light emitting diodes and full colour intelligent image displays to nano-transisitors and interconnects.

Acknowledgements

JDH is grateful to Prof Brian Robinson for the invitation to write this chapter and present his work at the 'Self-Assembly – The Future' conference in Massa Marritima in April 2002. The authors acknowledge financial support from the European Union under the Future and Emerging Technologies Programme (Project No. IST-2000-25469) and Intel (Ireland) Ltd. The authors thank Donal Lyons and Kirk Ziegler for their help in preparing this article.

References

[1] Timp, G. *Nanotechnology*; 1st ed.; Springer-Verlag: New York, 1999.
[2] Compano, R. *Technology Roadmap for Nanoelectronics*; European Communities: Brussels, 2000.
[3] Heath, J. R.; Kuekes, P. J.; Snider, G. S.; Williams, R. S. *Science* **1998**, *280*, 1716.
[4] Cui, Y.; Duan, X.; Hu, J.; Leiber, C. M. *J. Phys. Chem. B* **2000**, *104*, 5213.
[5] Yu, J.-Y.; Chung, S.-W.; Heath, J. R. *J. Phys. Chem. B* **2000**, *104*, 11864.
[6] Canham, L. T. *Appl. Phys. Lett.* **1990**, *57*, 1046.
[7] Tang, Y. H.; Zhang, Y. F.; Peng, H. Y.; Wang, N.; Lee, C. S.; Lee, S. T. *Chem. Phys. Lett.* **1999**, *314*, 16.
[8] Wu, Y.; Yang, P. *J. Am. Chem. Soc.* **2001**, *123*, 3165.
[9] Holmes, J. D.; Johnston, K. P.; Doty, R. C.; Korgel, B. A. S., 287, 1471. *Science* **2000**, *287*, 1471.
[10] Li, Y.; Xu, D.; Zhang, Q.; Chen, D.; Huang, F.; Xu, Y.; Guo, G.; Gu, Z. *Chem. Mater.* **1999**, *11*, 3433.
[11] Schmid, G.; Baumle, M.; Geerkens, M.; Heim, I.; Osemann, C.; Sawitowski, T. *Chem. Soc. Rev.* **1999**, *28*, 179.
[12] Schonenberger, C.; van der Zande, B. M. I.; Fokkink, L. G. J.; Henny, M.; Schmid, C.; Kruger, M.; Bachtold, A.; Huber, R.; Staufer, U. J. P. C. B., 101, 5497. *J. Phys. Chem. B* **1997**, *101*, 5497.
[13] Nguyen, P. P.; Pearson, D. H.; Tonucci, R. J.; Babcock, K. J. E. S., 145, 247. *J. Electrochem. Soc.* **1998**, *145*, 247.
[14] Cepak, V. M.; Hulteen, J. C.; Che, G.; Jirage, K. B.; Lakshmi, B. B.; Fischer, E. R.; Martin, C. R. *Chem. Mater.* **1997**, *9*, 1065.
[15] Cepak, V. M.; Martin, C. R. *J. Phys. Chem. B* **1998**, *102*, 9985.
[16] Martin, C. R. *Science* **1994**, *266*, 1961.
[17] Kresage, C. T.; Leonwicz, M. E.; Roth, W. J.; Vartuli, J. C.; Beck, J. S. *Nature* **1992**, *359*, 710.
[18] Leon, R.; Margolese, D.; Stucky, G.; Petroff, P. M. *Phys. Rev. B* **1995**, *52*, R2285.
[19] Dag, O.; Ozin, G. A.; Yang, H.; Reber, C.; Bussiere, G. *Adv. Mater.* **1999**, *11*, 474.
[20] Coleman, N. R. B.; Morris, M. A.; Spalding, T. R.; Holmes, J. D. J. A. C. S., 123, 187. *J. Am. Chem. Soc.* **2001**, *123*, 187.

[21] Coleman, N. R. B.; O'Sullivan, N.; Ryan, K. M.; Crowley, T. A.; Morris, M. A.; Spalding, T. R.; Steytler, D. C.; Holmes, J. D. *J. Am. Chem. Soc.* **2001**, *123*, 7010.
[22] Coleman, N. R. B.; Ryan, K. M.; Spalding, T. R.; Holmes, J. D.; Morris, M. A. *Chem. Phys. Lett.* **2001**, *343*, 1.
[23] Clifford, T. *Fundamentals of Supercritical Fluids*; 1st ed.; Oxford University Press: New York, 1998.
[24] Zhao, D.; Sun, J.; Li, Q.; Stucky, G. D. *Chem. Mater.* **2000**, *12*, 275.
[25] Attard, G. S.; Goltner, C. G. *Nature* **1995**, *378*, 366.
[26] Junges, U.; Jacobs, W.; Voight-Martin, I.; Krutzsch, B.; Schuth, F. *J. Chem. Soc. Chem. Commun.* **1995**, 2283.
[27] Ryan, K. M.; Coleman, N. R. B.; Lyons, D. M.; Morris, M. A.; Steytler, D. C.; Heenan, R. K.; Holmes, J. D. *Langmuir* **2002**, *18*, 4996.
[28] Steel, A.; Carr, S. W.; Anderson, M. W. *Chem. Mater.* **1995**, *7*, 1829.
[29] Koch, F.; Petrova-Koch, V.; Muschik, T.; Nikolov, A.; Gavrilenko, V. *Mater. Res. Soc. Symp. Proc* **1993**, *283*, 197.
[30] Littau, K. A.; Szajowski, P. F.; Muller, A. J.; Kortan, A. R.; Brus, L. E. *J. Phys. Chem.* **1993**, *97*, 1224.
[31] Glinka, Y. D.; Lin, S. H.; Huang, L. P.; Chen, Y. T.; Tolk, N. H. *Phys. Rev. B* **2001**, *64*, 5421.
[32] Ledoux, G.; Guillois, O.; Porterat, D.; Reynaud, C.; Huisken, F.; Kohn, B.; Paillard, V. *Phys. Rev. B* **2000**, *62*, 15942.
[33] Lyons, D. M.; Ryan, K. M.; Morris, M. A.; Holmes, J. D. *Nanolett.* **2002**, *2*, 811.
[34] Calcott, P. D. J.; Nash, K. J.; Canham, L. T.; Kane, M. J.; Brumhead, D. *J. Phys. Condens. Mater.* **1993**, *5*, L91.
[35] Qin, G. G.; Lin, J.; Duan, J. Q.; Yao, G. Q. *Appl. Phys. Lett.* **1996**, *69*, 1689.
[36] Yu, D. P.; Hang, H. L.; Ding, Y.; Zhang, H. Z.; Bai, Z. G.; Wang, J. J.; Zou, Y. H.; Qian, W.; Xiong, G. C.; Q., F. S. *Appl. Phys. Lett.* **1998**, *73*, 3076.
[37] Nishida, M. *Solid State Commun.* **2000**, *116*, 655.
[38] Liu, H. I.; Biegelsen, D. K.; Ponce, F. A.; Johnson, N. M.; Pease, R. F. W. *Appl. Phys. Lett.* **1994**, *64*, 1383.
[39] Harrington, P. A. *Synthesis and Characterisation of Dimensionally Ordered Copper Nanowires within Mesoporous Silica*; University College Cork: Cork, 2001, pp 30.
[40] Crowley, T. A. *Synthesis of Magnetic Nanowires within a Mesoporous Silica Matrix*; University College Cork: Cork, 2002, pp 78.
[41] Ng, W. L.; Lourenco, M. A.; Gwilliam, R. M.; Ledain, S.; Shao, G.; Homewood, K. P. *Nature* **2001**, *410*, 192.